PHILOSOPHICAL TRANSACTIONS OF THE ROYAL SOCIETY A MATHEMATICAL, PHYSICAL & ENGINEERING SCIENCES

Regional temperature and precipitation changes under high-end (≥4 °C) global warming

M. G. Sanderson, D. L. Hemming and R. A. Betts

Phil. Trans. R. Soc. A 2011 **369**, 85-98
doi: 10.1098/rsta.2010.0283

PHILOSOPHICAL TRANSACTIONS OF THE ROYAL SOCIETY A

Phil. Trans. R. Soc. A (2011) **369**, 85–98
doi:10.1098/rsta.2010.0283

Regional temperature and precipitation changes under high-end (≥4°C) global warming

By M. G. Sanderson*, D. L. Hemming and R. A. Betts

Met Office Hadley Centre, Fitzroy Road, Exeter EX1 3PB, UK

Climate models vary widely in their projections of both global mean temperature rise and regional climate changes, but are there any systematic differences in regional changes associated with different levels of global climate sensitivity? This paper examines model projections of climate change over the twenty-first century from the Intergovernmental Panel on Climate Change Fourth Assessment Report which used the A2 scenario from the IPCC Special Report on Emissions Scenarios, assessing whether different regional responses can be seen in models categorized as 'high-end' (those projecting 4°C or more by the end of the twenty-first century relative to the preindustrial). It also identifies regions where the largest climate changes are projected under high-end warming. The mean spatial patterns of change, normalized against the global rate of warming, are generally similar in high-end and 'non-high-end' simulations. The exception is the higher latitudes, where land areas warm relatively faster in boreal summer in high-end models, but sea ice areas show varying differences in boreal winter. Many continental interiors warm approximately twice as fast as the global average, with this being particularly accentuated in boreal summer, and the winter-time Arctic Ocean temperatures rise more than three times faster than the global average. Large temperature increases and precipitation decreases are projected in some of the regions that currently experience water resource pressures, including Mediterranean fringe regions, indicating enhanced pressure on water resources in these areas.

Keywords: regional climate change; precipitation; temperature; global climate models

1. Introduction

Global emissions of greenhouse gases have continued to rise, with an increasing trend, throughout the twentieth century and the first decade of the twenty-first century. This has occurred against a backdrop of almost two decades of political efforts to limit greenhouse gas emissions since the Rio Earth Summit in 1992. The Copenhagen Accord, agreed in December 2009, has a stated aim of limiting global warming to 2°C above preindustrial temperatures. This target may be

*Author for correspondence (michael.sanderson@metoffice.gov.uk).

One contribution of 13 to a Theme Issue 'Four degrees and beyond: the potential for a global temperature increase of four degrees and its implications'.

technically possible to achieve but will probably require substantial cuts in global greenhouse gas emissions in the very near future [1]. However, current national emissions-reduction pledges appear to be insufficient to keep global warming below 2°C [2].

Under scenarios of emissions in the absence of international climate policy, climate model projections assessed in the Intergovernmental Panel on Climate Change (IPCC) Fourth Assessment Report ([3]; henceforth referred to as AR4) indicate a range of global mean warming between 1.1°C and 6.4°C for 2090–2099, relative to 1980–1999. Global temperatures rose by about 0.5°C between the preindustrial period and 1980–1999; hence, current climate projections encompass a range of 1.6–6.9°C for the end of the twenty-first century, relative to the preindustrial period. Such changes would be expected to exert major impacts and stresses on physical and human systems worldwide [4,5]. However, there are significant differences and uncertainties among the various climate models and their projections, and current knowledge on the potential for and implications of such extreme climate changes over the twenty-first century is limited.

One key issue is whether changes in global mean temperature are a useful guide to changes in a particular region. Observational data and models agree that the world is not warming at a uniform rate across the globe, and this geographical variation in the rate of warming is expected to continue. There have been previous analyses of regional climate change from global climate projections and identification of areas most strongly affected. Giorgi & Bi [6] analysed temperature and precipitation changes for 26 land regions using an ensemble of global climate projections that were forced by the Special Report on Emissions Scenarios (SRES) A1B scenario [7]. They found that, in the model simulations, temperatures increased in all regions during the twenty-first century, and precipitation decreased the most in Central America, southern South America, the Mediterranean and northern Africa, Central Asia, southern Africa and Australia. Precipitation increased over most other land areas, showing that, generally, rainfall decreased over dry areas but increased over wetter areas. Further analyses by Giorgi & Bi [8] identified when precipitation changes outside of the range of model projections and variability occur in various regions. Baettig *et al.* [9] developed climate change indices to identify regions where large changes in temperature and precipitation might occur. Using results from three global climate models, their results (for precipitation) were in agreement with those of Giorgi & Bi [6], except over the Amazon, southern South America and Central Asia.

Some models project a faster rate of global warming than others, but it is not yet clear whether this involves systematic differences at the regional scale. This is an important issue as it could indicate whether a faster rate of warming could be associated with particular regional changes. This paper begins to address this question by analysing atmosphere–ocean global climate model (AOGCM) projections from the AR4. The range of projected global warming of 1.6–6.9°C was from a wide set of emission scenarios examined with a number of different types of models, including AOGCMs, simple climate models and Earth system models (including both GCMs and simple models incorporating biogeochemical feedbacks). This paper focuses on a subset of these projections, specifically the AR4 AOGCM simulations driven by a single emissions scenario (the SRES A2 scenario; [7]).

In §2, the methodology is described. Next, the magnitudes and patterns of climate change from high-end model simulations are examined and compared with the remaining projections, to see whether the behaviour of these two classes of model is very different. We then identify areas experiencing the greatest impacts of high-end climate change, which are those regions where the largest changes in temperature and precipitation occur.

2. Methodology

The AR4 ensemble of global climate model projections was forced with greenhouse gas concentrations inferred from several SRES emissions scenarios [7]. The emissions of greenhouse gases (and hence greenhouse gas concentrations in the atmosphere) are greatest in the A2 scenario. Gridded temperature and precipitation data from each model were obtained from the Programme for Climate Model Diagnosis and Intercomparison (PCMDI; http://www-pcmdi.llnl.gov). The models use many different horizontal grids; to facilitate comparison and analysis, all model results were transformed to the same horizontal resolution (1.875° longitude by 1.25° latitude) as the HadGEM1 model [10]. Here, we focused on the set of projections for the A2 scenario, to allow investigation of the variations in climate model responses to a single scenario of greenhouse gas concentrations. Of the 24 models discussed in the AR4, 19 were forced with the A2 scenario. Multiple simulations using the A2 scenario were available for some models (which differed only in the initial conditions used), in which case each simulation was treated independently. Overall, 40 simulations using the A2 scenario were available for our analysis. The models and simulations are listed in table 1.

Additionally, all models had been used to perform a preindustrial control experiment, where greenhouse gas concentrations were held at fixed levels throughout the simulation. We plotted time series of global annual mean temperatures calculated from the preindustrial simulations and examined them by eye. Any clear initial drift in the temperatures (resulting from the modelled climate adjusting from its initial state to that determined by the greenhouse gas concentrations) was identified, and that portion of the data was not included in the analysis. It was only necessary to exclude some of these data for a few of the models. Preindustrial mean temperatures were then calculated from the remaining years (which numbered between 180 and 940).

The increase in global mean temperatures between the preindustrial and the period 2090–2099 was calculated for all 40 simulations and rounded to one decimal point. In order to separate the simulations into those that warm faster and those that warm slower under a given forcing, we used an increase in global mean temperature of 4°C relative to preindustrial as an indicator. We classed those simulations that projected 4°C or more as 'high-end'. There are too few results to assign probabilities to the changes; although appropriate methods to calculate probabilities are available (e.g. [11]), they are outside the scope of this paper. Internal variability in the models will not have a significant impact on the analysis, because simulated climate change by the 2090s will be dominated by the modelled response to the increasing greenhouse gas concentrations. These simulations suggest that a warming of 4°C could be reached from the 2080s [12].

Table 1. AR4 models analysed. Only those models which were run using the SRES A2 scenario are listed. The columns headed 'run no.' contain the number of the simulation analysed. The change in annual mean temperature for each simulation between the preindustrial period and 2090–2099 is given in the columns headed 'ΔT(°C)'. Simulations classed as high-end (which are 4.0°C or greater) are shown in italics.

model	run no.	ΔT(°C)	model	run no.	ΔT(°C)
bccr_bcm_2	1	3.7	miub_echo_g	3	*4.0*
cccma_cgcm3_1	1	*4.5*	mpi_echam5	1	*4.0*
cccma_cgcm3_1	2	*4.5*	mpi_echam5	2	*4.0*
cccma_cgcm3_1	3	*4.5*	mpi_echam5	3	*4.0*
cccma_cgcm3_1	4	*4.4*	mri_cgcm2_3_2a	1	3.3
cccma_cgcm3_1	5	*4.4*	mri_cgcm2_3_2a	2	3.4
cnrm_cm3	1	*4.9*	mri_cgcm2_3_2a	3	3.3
csiro_mk3_0	1	3.4	mri_cgcm2_3_2a	4	3.4
csiro_mk3_5	1	*4.4*	mri_cgcm2_3_2a	5	3.4
gfdl_cm2_0	1	3.6	ncar_ccsm3_0	1	*4.3*
gfdl_cm2_1	1	3.6	ncar_ccsm3_0	2	*4.2*
giss_model_e_r	1	3.0	ncar_ccsm3_0	3	*4.2*
ingv_echam4	1	3.7	ncar_ccsm3_0	4	*4.2*
inmcm3_0	1	3.8	ncar_ccsm3_0	5	*4.2*
ipsl_cm4	1	*4.5*	ncar_pcm1	1	3.1
miroc3_2_medres	1	*4.0*	ncar_pcm1	2	3.0
miroc3_2_medres	2	3.9	ncar_pcm1	3	3.0
miroc3_2_medres	3	3.9	ncar_pcm1	4	3.1
miub_echo_g	1	3.8	ukmo_hadcm3	1	*4.0*
miub_echo_g	2	*4.0*	ukmo_hadgem1	1	*4.8*

3. Results

Overall, 21 projections using the A2 scenario were classed as high-end, and 19 as non-high-end. Temperature increases in several of the non-high-end projections reached 4°C or more during the 2090s in individual years. However, their decadal average temperature increases for the 2090s were less than 4°C, and so those models were not classed as high-end. Temperature increases from all simulations are given in table 1, where those from the high-end projections are in italics. In a similar analysis to that of Räisänen [13], the correlation between the temperature change and the modelled preindustrial mean temperature for all projections was calculated. Only the models that simulate the large areas of ice in the polar regions, which will have the coldest temperatures for the preindustrial period, can produce a large warming as the ice sheets recede. However, no correlation was observed, indicating that any relationship between modelled preindustrial ice sheet extent and temperature increases is complex and nonlinear.

Next, regional changes in temperature and precipitation in the high-end and non-high-end models are examined. To minimize any impacts of decadal variability, model results for 2070–2099 are analysed. The median changes in temperature and precipitation for December, January and February (DJF)

and June, July and August (JJA), averaged over the period 2070–2099, were calculated from the high-end and non-high-end projections together with the maximum range from each group of models. Median values are used instead of the mean, because mean values are subject to bias from models that produce very large or very small changes that could be considered as outliers.

It is possible that the regional patterns of warming in the high-end and non-high-end models are similar, but are simply larger in magnitude in the high-end models. To focus on the regional responses, for each simulation, we normalized the local warming in each grid box by dividing by the global mean warming. This normalization was done separately for DJF and JJA. This approach assumes that the response of the models to global temperature change is linear, which has been shown to be a reasonable assumption [14]. The resulting patterns shown in figures 1 and 2 are the median regional temperature responses simulated by the models per degree of global mean temperature increase (colour-shaded contours) and the 5th–95th percentile range of temperature changes from each set of models (solid contours with labels).

The largest normalized regional temperature changes occur during DJF and are located over much of the Arctic for both high-end and non-high-end models (figure 1*a*,*b*) and have very similar magnitudes. These changes are much greater than those for JJA (figure 2*a*,*b*). The largest increases in DJF occur over Canada and the northern half of Asia and are about 4°C per 1°C of global warming. This large temperature increase at high northern latitudes is caused by the loss of ice and reduced winter snow coverage, exposing land and oceans which will absorb large amounts of incoming solar radiation (which will act to amplify the warming). Additionally, there will also be changes in the poleward energy transport, which is simulated to increase with rising temperature [15]. However, the range of temperature changes in the Arctic from the models is similar to or larger than the actual temperature change (figure 1*a*,*b*, solid contours with labels). Climate models are known to have large biases in their simulations of ice and snow cover over high northern latitudes. Models that simulate a large amount of snow and ice for the present-day climate are likely to simulate a large degree of warming in this region as the ice retreats. Models that simulate lower ice coverage in the Arctic will produce a smaller amount of warming [13]. The magnitude and inter-model range of simulated warming over high northern latitudes are very similar in the high-end and non-high-end models, which indicates that the biases among the models are larger than the climate change signal.

Figure 1*c* shows the difference between the normalized high-end and non-high-end temperature changes for DJF. A positive value indicates that the high-end models are warmer than the non-high-end models. The high-end models are colder by 0.5°C per 1°C global warming or more over the northeastern edge of Europe and the nearby Arctic regions, and around the northern parts of Japan. They simulate warmer temperatures around the coasts of Canada, Alaska, Greenland and the Arctic region of Asia. Warmer areas are also simulated by the high-end models over Central Asia, the northern coast of South America and northwestern Australia. Overall, the pattern-scaled temperature changes in the high-end and non-high-end models are similar over much of the globe, but there are some regional differences, indicating that the regional response of the high-end and non-high-end models to climate change is not completely identical.

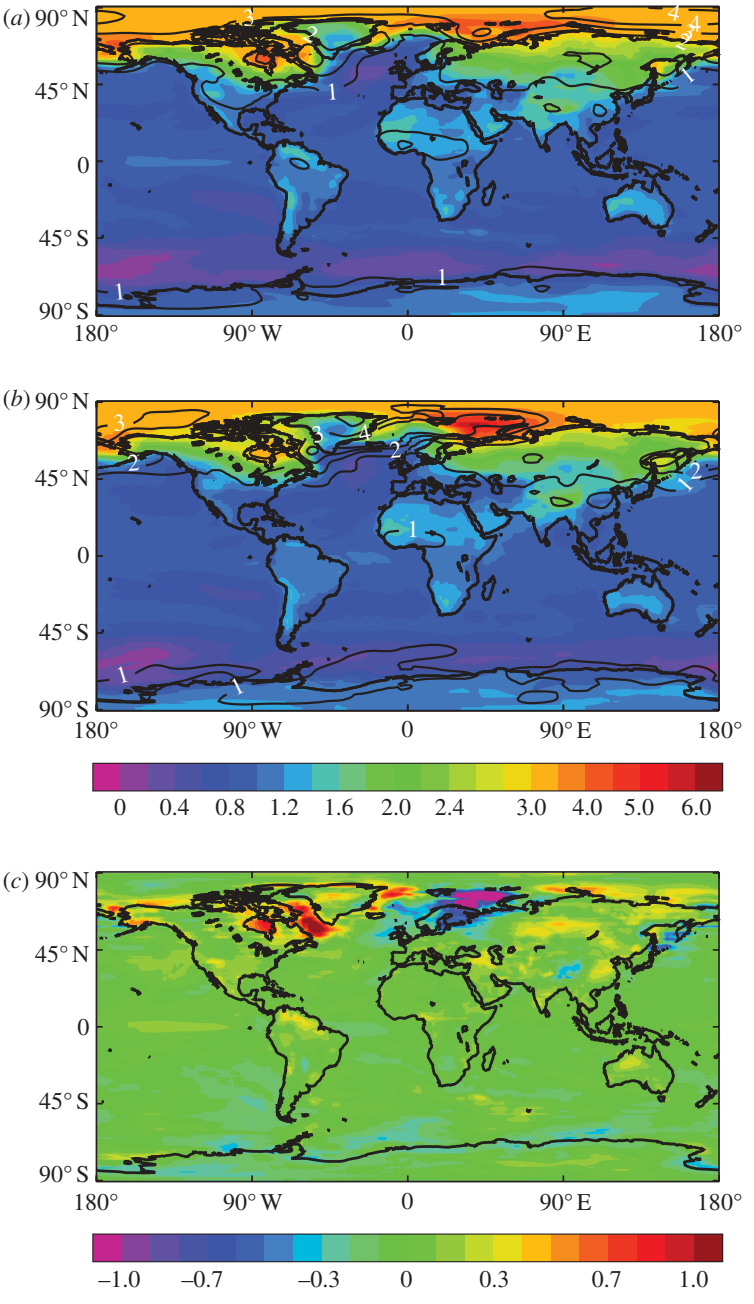

Figure 1. Median temperature responses simulated by the models per degree of global mean temperature increase for DJF. (*a*) Median temperature changes from the high-end members, shown by the colour-shaded contours. The solid contours with labels show the range of temperature changes across the high-end models (again scaled by the global mean temperature rise). Note that the temperature scale changes at 3°C. (*b*) As (*a*), but for the non-high-end members. (*c*) Difference between the medians of the high-end and non-high-end members. A positive value indicates that the scaled temperatures in the high-end models are warmer than the non-high-end models.

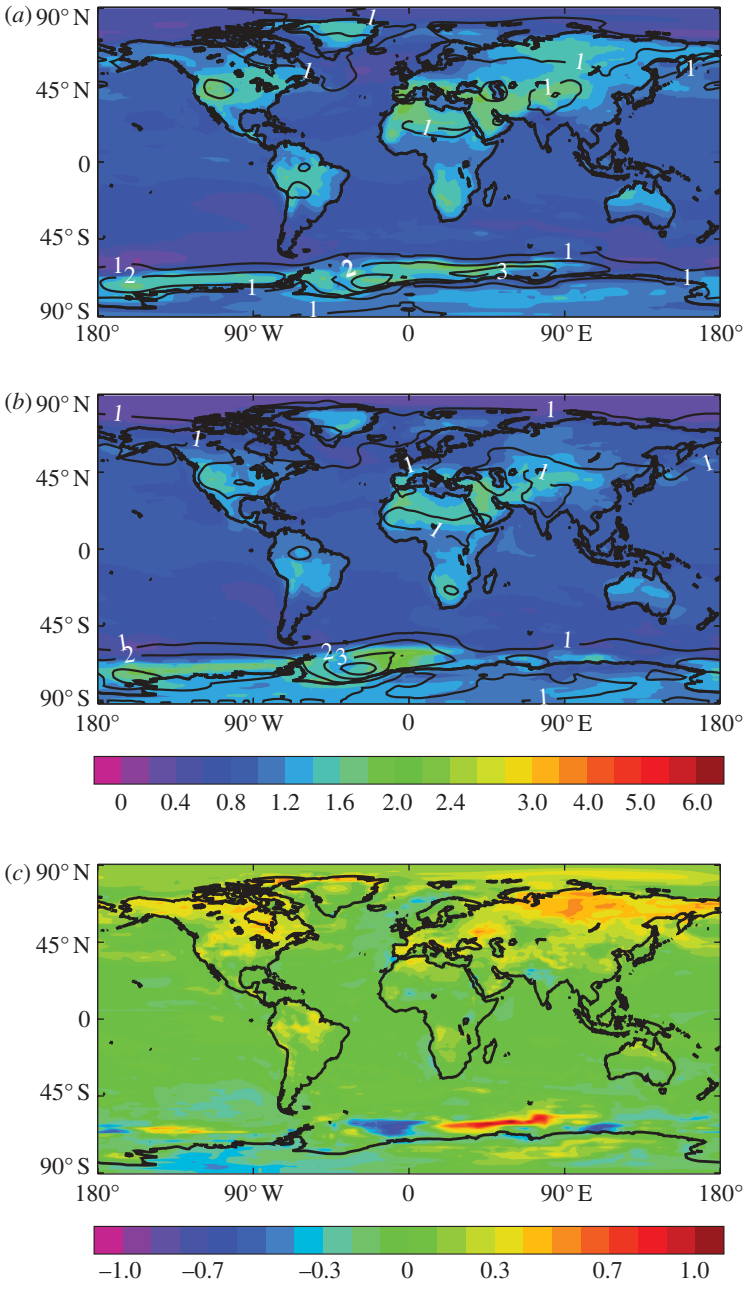

Figure 2. Median temperature responses simulated by the models per degree of global mean temperature increase for JJA. (*a*) Median temperature changes from the high-end members, shown by the colour-shaded contours. The solid contours with labels show the range of temperature changes across the high-end models (again scaled by the global mean temperature rise). Note that the temperature scale changes at 3°C. (*b*) As (*a*), but for the non-high-end members. (*c*) Difference between the (scaled) medians of the high-end and non-high-end members. A positive value indicates that the temperatures in the high-end models are warmer than the non-high-end models.

An area of water where almost no warming occurs is projected to form in the northern North Atlantic, between the UK and Greenland, and this area is larger in the high-end models. This cooler water could be caused by a slowing of the North Atlantic thermohaline circulation [4]. None of the models analysed by the IPCC [4] simulates an increase in this circulation with a warming climate, and the modelled response varies between essentially no change and a 50 per cent reduction. There may also be increased deep vertical mixing in the high-end models, which acts to warm waters well below the surface but reduces the surface warming [13]. A similar area of water is also projected to form over much of the Southern Ocean. The spatial extent of this cooler water is larger in the high-end models than in the non-high-end models. The temperature range across the models in the Arctic and Antarctic regions is of a magnitude similar to or larger than the median change, indicating that biases resulting from differences in modelled ice and snow amounts are similar to or larger than the climate change response [16].

In JJA, the largest differences in normalized regional temperature changes between the high-end and non-high-end members occur over land and are mostly confined to smaller areas between 45° N and 45° S (figure 2*a*,*b*). The magnitude of these temperature changes is smaller than those seen for DJF. The land–ocean temperature contrast is also larger than in DJF. Enhanced warming is seen over much of the USA, parts of South America, the Mediterranean areas, northern and southern Africa, Central Asia and parts of northern Australia (colour-shaded contours). This normalized warming generally lies between 1.4°C and 2°C per 1°C global warming. The 5th–95th percentile temperature range across the models (shown by solid contours with labels) in these regions is smaller and has a different spatial pattern, suggesting that these simulated patterns of warming are not largely controlled by model biases. A small area with a high degree of warming is simulated around the coast of Antarctica, where the inter-model temperature range is also large. Again, this area of warming is likely to result from biases in modelled sea ice amounts [16]. The difference in scaled temperatures between the high-end and non-high-end models is shown in figure 2*c*. The high-end models project normalized regional warming, which is 0.2–0.6°C per 1°C global warming greater over much of the Northern Hemisphere land masses. Smaller areas of relatively faster regional warming are also seen over South America, southern Africa and Australia. This difference could be due to larger poleward energy transport in the high-end models, which is simulated to increase with warmer temperatures [15].

A small area of less warm water in the North Atlantic Ocean is simulated for JJA, and the warming is slightly greater than in DJF. Around Antarctica, both positive and negative differences in warming between the high-end and non-high-end models are seen. These differences are likely to be due to variations in the modelled responses of the sea ice.

Overall, the patterns of the response of regional climate to global climate change in the high-end and non-high-end models are similar during DJF and JJA. However, the regional response of the high-end models is larger, particularly during JJA. Much of the warming seen during DJF over high northern latitudes is strongly controlled by each model's simulation of ice and snow cover during the preindustrial period, and how they respond to a warming climate. Models are known to have large biases in snow and ice cover over high northern latitudes [16].

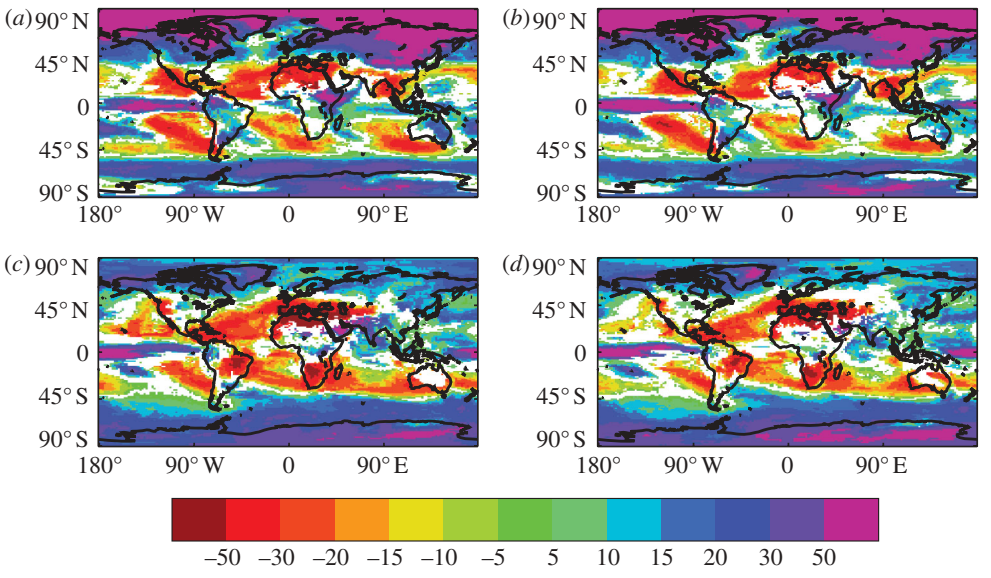

Figure 3. Precipitation changes (%) in (*a*,*b*) DJF and (*c*,*d*) JJA from the median of the A2 ensemble, after scaling to 4°C global mean warming in all cases. (*a*,*c*) Precipitation changes from the high-end members, and (*b*,*d*) changes from the non-high-end members. The data are only shown where 66% or more of the models agree on the sign of the change.

Maps illustrating the percentage changes in precipitation during DJF and JJA for the high-end and non-high-end members are shown in figure 3. It has been shown that the patterns of regional temperature response of the high-end and non-high-end models to climate change are similar, although the temperature response of the high-end models tended to be greater. The precipitation changes from each model were scaled to a global mean temperature rise of 4°C. Previous work [17] has shown that global precipitation in most models increases linearly with increasing temperature. By scaling the precipitation changes, the maps shown in figure 3 will illustrate any differences between the precipitation responses of the high-end and non-high-end models. The precipitation changes have only been plotted if 66 per cent or more of the models agree on the sign of the change. White areas in figure 3 are where fewer than 66 per cent of the models agree on the sign of the change, and thus represent locations where there is no reliable signal.

Areas experiencing large decreases in precipitation are evident in both DJF and JJA, in both the high-end and non-high-end members, and occur between 50° N and 50° S. The patterns in each season are very similar between the high-end and non-high-end models, but the precipitation decreases are larger in magnitude in some regions in the high-end models than in the non-high-end models. The total area (land and ocean) where precipitation decreases is also larger in the high-end models than in the non-high-end models, by 14 per cent in DJF and 7 per cent in JJA. In DJF, precipitation is projected to decrease over Central America, the Mediterranean, northern Africa, India and parts of Southeast Asia. Other regions experiencing a decrease in rainfall are the southernmost parts of

South America and much of Chile. Precipitation is projected to increase over most of the remainder of South America, the Horn of Africa and much of Australia. Precipitation is projected to increase over almost all areas north of 45° N and south of 50° S.

During JJA, the area of Europe experiencing a precipitation decrease has extended northwards to cover most of the continent, except Scandinavia. Precipitation is still projected to decrease over Central America, and also to decrease over large parts of Brazil, southern Africa and Australia. Increases in JJA precipitation are projected over India and Southeast Asia. There is poor model agreement over much of the USA and Australia during JJA.

The differences in precipitation changes between the high-end and non-high-end models in DJF and JJA were also investigated (data not shown). The differences are very small over most regions (less than ±5%), except for a small area of the equatorial Pacific Ocean, where the non-high-end models project an increase in precipitation that is about 50 per cent greater than in the high-end models. There were also a few small areas over northern Africa, Alaska and the adjacent part of eastern Russia (Chukotka) where larger precipitation changes in the high-end models were projected, but these areas are small.

The increases in precipitation seen at higher latitudes are a result of increasing amounts of water vapour in the atmosphere. Warmer temperatures result in higher evaporation rates, and warmer air can hold more water vapour. There is also an increasing poleward transport of water vapour from lower latitudes. The subtropical regions (e.g. the Mediterranean, North Africa and Central America) experience a drying owing to increased transport of water vapour out of this area and an expansion of the subtropical high-pressure regions towards the poles [4]. In these regions, the air is very dry and the high pressures suppress precipitation.

Over Europe and the adjacent parts of central western Asia, the areas with enhanced warming in the high-end models are similar to the areas where the precipitation has decreased. This result suggests that the reduced precipitation has caused drier soils, which in turn have enhanced the warming owing to reduced cooling by evaporation. The areas with enhanced warming over the USA may also be caused by drier soils from reduced precipitation, although the poor model agreement in precipitation changes for this region means this conclusion is uncertain. The warming over southern Africa may also be a result of reduced precipitation. The JJA precipitation decreases by 20–50% in this region for a 4°C global warming, where enhanced warming is also seen.

The regions that could be most strongly affected by high-end climate change are now identified. These regions are defined as those where temperatures increase by at least 6°C and precipitation changes by at least 10 per cent, for 4°C global warming. These limits are arbitrary but are likely to have a large impact on ecosystems [5]. Temperature and precipitation changes from the high-end model simulations (21 runs) were scaled to a global mean warming of 4°C. Although there will be some nonlinearities in the modelled responses, they are unlikely to be large enough to affect the results [14].

The regions most strongly affected by high-end climate change are shown in figure 4. The colours indicate regions where both the temperature and precipitation changes are equal to or exceed the limits given in the previous

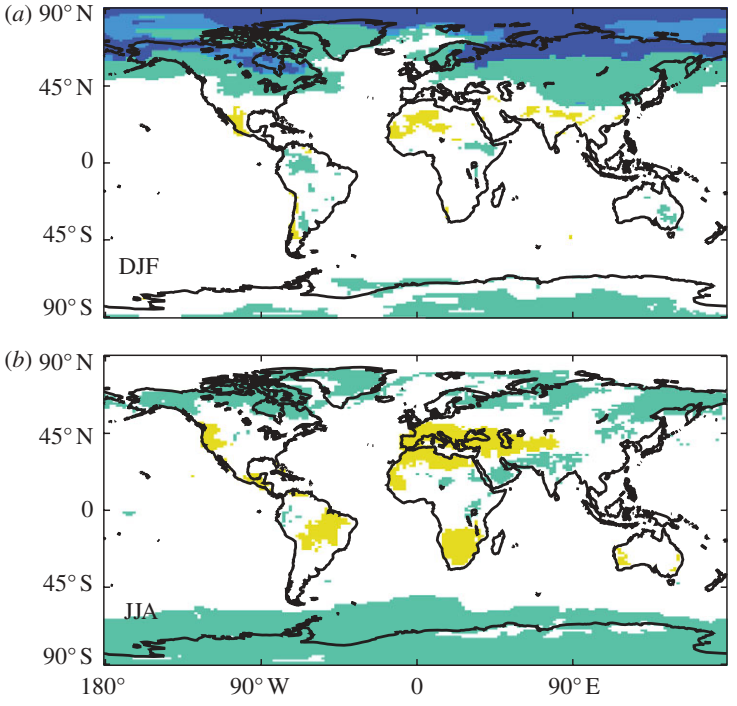

Figure 4. Areas most strongly affected by high-end climate change in (*a*) DJF and (*b*) JJA. The temperature and precipitation changes from the high-end models were scaled to a global mean warming of 4°C. The coloured areas indicate where precipitation changes by at least ±10% and temperature increases by at least 6°C for 4°C global warming. Yellow colour indicates areas where precipitation decreases, and at least 66% of the models agree on the sign of the change. Light green, light blue and dark blue colours show areas where precipitation increases by 10% or more for 4°C global warming. The light green colour areas show where one or more models project a temperature rise of at least 6°C, and at least 66% of the models project a precipitation increase. The blue colours indicate regions where all models project a temperature rise of at least 6°C, and 90% (light blue) or 100% (dark blue) of the models agree on the sign of the precipitation change.

paragraph. Light green, light blue and dark blue colours show areas where precipitation increases by 10 per cent or more for 4°C global warming. The light green areas show where one or more models project a temperature rise of at least 6°C, and at least 66 per cent of the models project a precipitation increase. The blue colours indicate regions where all models project a temperature rise of at least 6°C, and 90 per cent (light blue) or 100 per cent (dark blue) of the models agree on the sign of the precipitation change. The green and blue colours, therefore, represent the minimum (dark blue) and maximum (all green and blue colours) extent of regions projected to experience temperature and precipitation increases above the limits set earlier. The yellow areas in figure 4 indicate those regions where precipitation decreases by 10 per cent or more, at least 66 per cent of the models agree on the sign of the change and all models project a temperature rise of 6°C or more.

For DJF (figure 4*a*), the spatial extent of the maximum and minimum areas projected to experience the highest climate changes under a global warming of 4°C is very different, highlighting the uncertainty that mostly originates from the different temperature changes projected by the models. There are smaller regions (Mexico, northern Africa and parts of Southeast Asia) shown in yellow where there is reasonable confidence that precipitation will decrease.

For JJA (figure 4*b*), Central America, parts of Brazil, southern Africa, and parts of Europe, northern Africa and the adjacent part of Central Asia are projected to suffer large rises in temperature and decreased precipitation. Small parts of the USA and Australia could be similarly affected. Much of the high northern latitude regions are projected to receive increases in precipitation together with large temperature rises. Other locations (the Arabian Peninsula, parts of northern India) may also change in the same way, but the areas are small. There are no regions during JJA where the temperature rises by 6°C, and 90 per cent or more of the models agree on the sign of the precipitation change (if that change is at least 10%). For JJA, the uncertainty in the projections mostly originates from differences in modelled precipitation changes.

4. Conclusions

Forty global climate model projections using the A2 scenario from the IPCC Fourth Assessment Report have been analysed, and a number of simulations that project a high-end warming of 4°C or more by the 2090s (relative to the preindustrial period) were found. About half of the simulations were classed as high-end. Under the high-end models, Northern Africa is projected to experience high (greater than 6°C) temperature increases and large precipitation decreases in both DJF and JJA, suggesting that this region is most at risk from high-end climate change. In addition, during JJA, Southern Europe and the adjacent part of Central Asia are projected to warm by 6–8°C, together with a decrease in precipitation of 10 per cent or more. This result suggests that drier soils, a consequence of the reduced precipitation, are the cause of the elevated temperatures, as the evaporative cooling effect will be smaller. The large-scale patterns of temperature and precipitation change in the high-end and non-high-end projections are similar, although the magnitudes of temperature change were larger in the high-end models, especially during JJA. The main difference in the regional temperature response of the high-end models from the non-high-end models occurs over much of the Northern Hemisphere land areas during JJA. The high-end models project enhanced warming over most of northern Asia, Canada and the USA. The patterns and magnitude of the precipitation changes (scaled to a global mean warming of 4°C) are similar in the high-end and non-high-end models, although the reductions in precipitation tend to be slightly greater in the high-end models.

The regions where the greatest climate changes occur under 4°C global warming were identified using results from the high-end models. These regions are defined as those where temperatures increase by at least 6°C and precipitation changes by at least 10 per cent. During DJF, high northern latitude land areas, Mexico and parts of northern Africa are identified. For JJA, the largest climate

changes occur in northern and southern Africa, southern Europe and the adjacent part of Central Asia and parts of Brazil. The uncertainty in the regions affected by high-end climate change during DJF (the Arctic) is mostly due to differences in modelled temperature increases, which are caused by biases in simulated ice sheet extent and snow cover. However, for JJA, the uncertainty mostly originates from differences in modelled precipitation changes.

Much of the uncertainty in these results originates from the poor agreement in temperature and precipitation changes between the models in some areas. If agreement in these changes from the next generation of climate models, which will be used for the forthcoming IPCC Fifth Assessment Report, is greater, this work could be repeated to highlight other areas that could be strongly affected by high-end climate change. Further work could consider changes in extreme temperatures and precipitation.

This work was supported by the Joint DECC and Defra Integrated Climate Programme—DECC/Defra (GA01101). The authors also thank the various research groups for providing their model data, and the PCMDI for archiving the data.

References

1 Meinshausen, M., Meinshausen, N., Hare, W., Raper, S. C. B., Frieler, K., Knutti, R., Frame, D. J. & Allen, M. R. 2009 Greenhouse-gas emission targets for limiting global warming to 2°C. *Nature* **458**, 1158–1162. (doi:10.1038/nature08017)

2 Rogelj, J., Nabel, J., Chen, C., Hare, W., Markmann, K., Meinshausen, M., Schaeffer, M., Macey, K. & Höhne, N. 2010 Copenhagen Accord pledges are paltry. *Nature* **464**, 1126–1128. (doi:10.1038/4641126a)

3 IPCC. 2007 Summary for policymakers. In *Climate Change 2007: The Physical Science Basis. Contribution of Working Group I to the 4th Assessment Report of the Intergovernmental Panel on Climate Change* (eds S. Solomon, D. Qin, M. Manning, Z. Chen, M. Marquis, K. B. Averyt, M. Tignor & H. L. Miller). Cambridge, UK: Cambridge University Press.

4 Meehl, G. A. *et al.* 2007 Global climate projections. In *Climate Change 2007: The Physical Science Basis. Contribution of Working Group I to the 4th Assessment Report of the Intergovernmental Panel on Climate Change* (eds S. Solomon, D. Qin, M. Manning, Z. Chen, M. Marquis, K. B. Averyt, M. Tignor & H. L. Miller). Cambridge, UK: Cambridge University Press.

5 Fischlin, A. *et al.* 2007 Ecosystems, their properties, goods and services. In *IPCC 2007. Impacts, Adaptation and Vulnerability. Contribution of Working Group II to the 4th Assessment Report of the Intergovernmental Panel on Climate Change* (eds M. L. Parry, O. F. Canziani, J. P. Palutikof, P. J. van der Linden & C. E. Hanson). Cambridge, UK: Cambridge University Press.

6 Giorgi, F. & Bi, X. 2005 Updated regional precipitation and temperature changes for the 21st century from ensembles of recent AOGCM simulations. *Geophys. Res. Lett.* **32**, L21715. (doi:10.1029/2005GL024288)

7 IPCC. 2000 *Special Report on Emissions Scenarios* (eds N. Nakicenovic & R. Swart). Cambridge, UK: Cambridge University Press.

8 Giorgi, F. & Bi, X. 2009 Time of emergence (TOE) of GHG-forced precipitation change hot-spots. *Geophys. Res. Lett.* **36**, L06709. (doi:10.1029/2009GL037593)

9 Baettig, M. B., Wild, M. & Imboden, D. M. 2007 A climate change index: where climate change may be most prominent in the 21st century. *Geophys. Res. Lett.* **34**, L01705. (doi:10.1029/2006GL028159)

10 Johns, T. C. *et al.* 2006 The new Hadley centre climate model HadGEM1: evaluation of coupled simulations. *J. Clim.* **19**, 1327–1353. (doi:10.1175/JCLI3712.1)

11 Murphy, J. M., Booth, B. B. B., Collins, M., Harris, G. R., Sexton, D. M. H. & Webb, M. J. 2007 A methodology for probabilistic predictions of regional climate change from perturbed physics ensembles. *Phil. Trans. R. Soc. A* **365**, 1993–2028. (doi:10.1098/rsta.2007.2077)

12 Betts, R. A., Collins, M., Hemming, D. L., Jones, C. D., Lowe, J. A. & Sanderson, M. G. 2011 When could global warming reach 4°C? *Phil. Trans. R. Soc. A* **369**, 67–84. (doi:10.1098/rsta.2010.0292)
13 Räisänen, J. 2007 How reliable are climate models? *Tellus* **59A**, 2–29.
14 Mitchell, T. D. 2003 Pattern scaling: an examination of the accuracy of the technique for describing future climates. *Clim. Change* **60**, 217–242. (doi:10.1023/A:1026035305597)
15 Caballero, R. & Langen, P. L. 2005 The dynamic range of poleward energy transport in an atmospheric general circulation model. *Geophys. Res. Lett.* **32**, L02705. (doi:10.1029/2004GL021581)
16 Knutti, R., Furrer, R., Tebaldi, C., Cermak, J. & Meehl, G. A. 2010 Challenges in combining projections from multiple climate models. *J. Clim.* **23**, 2739–2758. (doi:10.1175/2009JCLI3361.1)
17 Lambert, F. H. & Webb, M. J. 2008 Dependency of global mean precipitation on surface temperature. *Geophys. Res. Lett.* **35**, L16706. (doi:10.1029/2008GL034838)